A climbing image nudged elastic band method for finding saddle points and minimum energy paths

Graeme Henkelman, Blas P. Uberuaga, and Hannes Jónsson

Citation: J. Chem. Phys. **113**, 9901 (2000); doi: 10.1063/1.1329672
View online: http://dx.doi.org/10.1063/1.1329672
View Table of Contents: http://jcp.aip.org/resource/1/JCPSA6/v113/i22
Published by the American Institute of Physics.

A climbing image nudged elastic band method for finding saddle points and minimum energy paths

Graeme Henkelman
Department of Chemistry 351700, University of Washington, Seattle, Washington 98195-1700

Blas P. Uberuaga
Department of Chemistry 351700, University of Washington, Seattle, Washington 98195-1700 and Department of Physics 351560, University of Washington, Seattle, Washington 98195-1560

Hannes Jónsson
Department of Chemistry 351700, University of Washington, Seattle, Washington 98195-1700

(Received 23 August 2000; accepted for publication 10 October 2000)

A modification of the nudged elastic band method for finding minimum energy paths is presented. One of the images is made to climb up along the elastic band to converge rigorously on the highest saddle point. Also, variable spring constants are used to increase the density of images near the top of the energy barrier to get an improved estimate of the reaction coordinate near the saddle point. Applications to CH_4 dissociative adsorption on Ir(111) and H_2 on Si(100) using plane wave based density functional theory are presented. © *2000 American Institute of Physics.* [S0021-9606(00)71246-3]

I. INTRODUCTION

An important problem in theoretical chemistry and condensed matter physics is the calculation of transition rates, for example rates of chemical reactions or diffusion events. Most often, it is sufficient to treat the motion of the atoms using classical mechanics, but the transitions of interest are typically many orders of magnitude slower than vibrations of the atoms, so a direct simulation of the classical dynamics is not feasible. For a process with a typical, low activation energy of 0.5 eV, the computer time required to simulate a classical trajectory long enough that a single transition event can be expected to occur is on the order of 10^4 years on present day computers. This ''rare event'' problem is devastating for direct dynamical simulations, but makes it possible to obtain accurate estimates of transition rates using a purely statistical approach, namely, transition state theory (TST).[1–4] Apart from the Born–Oppenheimer approximation, TST relies on two basic assumptions: (a) the rate is slow enough that a Boltzmann distribution is established and maintained in the reactant state and (b) a dividing surface of dimensionality D-1, where D is the number degrees of freedom in the system, can be identified such that a reacting trajectory going from the initial state to the final state only crosses the dividing surface once. The dividing surface must, therefore, represent a bottleneck for the transition.

Since atoms in crystals are usually tightly packed and the typical temperature of interest is low compared with the melting temperature, the harmonic approximation to TST (hTST) can typically be used in studies of diffusion and reactions in crystals or at crystal surfaces.[5] This greatly simplifies the problem of estimating the rates. The search for the optimal transition state then becomes a search for the lowest few saddle points at the edge of the potential energy basin corresponding to the initial state. The rate constant for transition through the region around each one of the saddle points can be obtained from the energy and frequency of normal modes at the saddle point and the initial state,[6,7]

$$k^{\mathrm{hTST}}=\frac{\Pi_i^{3N}\nu_i^{\mathrm{init}}}{\Pi_i^{3N-1}\nu_i^{\ddagger}}\,e^{-(E^{\ddagger}-E^{\mathrm{init}})/k_BT}. \tag{1}$$

Here, $E^{\ddagger}$ is the energy of the saddle point, E^{init} is the local potential energy minimum corresponding to the initial state, and the ν_i are the corresponding normal mode frequencies. The symbol ‡ refers to the saddle point. All the quantities can be evaluated from the potential energy surface, at zero temperature, but entropic effects are included through the harmonic approximation. The most challenging part in this calculation is the search for the relevant saddle point.

A path connecting the initial and final states that typically has the greatest statistical weight is the minimum energy path (MEP). At any point along the path, the force acting on the atoms is only pointing along the path. The energy is stationary for any perpendicular degree of freedom. The maxima on the MEP are saddle points on the potential energy surface. The relative distance along the MEP is a natural choice for a reaction coordinate, and at the saddle point the direction of the reaction coordinate is given by the normal mode eigenvector corresponding to negative curvature.

The MEP often has one or more minima in addition to the minima at the initial and final states. These correspond to stable intermediate configurations. The MEP will then have two or more maxima, each one corresponding to a saddle point. Assuming a Boltzmann population is reached for the intermediate (meta)stable configurations, the overall rate is determined by the *highest* saddle point. It is, therefore, not sufficient to find a saddle point. One needs to have a good enough estimate of the shape of the MEP to be able to assign the highest saddle point as ‡ in Eq. (1) in order to get an accurate estimate of the rate.

Many different methods have been presented for finding MEPs and saddle points.[8–10] Since a first order saddle point is a maximum in one direction and a minimum in all other directions, methods for finding saddle points invariably involve some kind of maximization of one degree of freedom and minimization in other degrees of freedom. The critical issue is to find a good and inexpensive way to decide which degree of freedom should be maximized.

The nudged elastic band (NEB) method is an efficient method for finding the MEP between a given initial and final state of a transition.[9,11,12] It has become widely used for estimating transition rates within the hTST approximation. The method has been used both in conjunction with electronic structure calculations, in particular plane wave based DFT calculations (see, for example, Refs. 13–17), and in combination with empirical potentials.[18–21] Studies of very large systems, including over a million atoms in the calculation, have been conducted.[22] The MEP is found by constructing a set of images (replicas) of the system, typically on the order of 4–20, between the initial and final state. A spring interaction between adjacent images is added to ensure continuity of the path, thus mimicking an elastic band. An optimization of the band, involving the minimization of the force acting on the images, brings the band to the MEP.

An essential feature of the NEB method, which distinguishes it from other elastic band methods,[23–25] is a force projection which ensures that the spring forces do not interfere with the convergence of the elastic band to the MEP, as well as ensuring that the true force does not affect the distribution of images along the MEP. It is necessary to estimate the tangent to the path at each image and every iteration during the minimization, in order to decompose the true force and the spring force into components parallel and perpendicular to the path. Only the perpendicular component of the true force is included, and only the parallel component of the spring force. This force projection is referred to as ''nudging.'' The spring forces then only control the spacing of the images along the band. When this projection scheme is not used, the spring forces tend to prevent the band from following a curved MEP (because of ''corner-cutting''), and the true force along the path causes the images to slide away from the high energy regions towards the minima, thereby reducing the density of images where they are most needed (the ''sliding-down'' problem). In the NEB method, there is no such competition between the true forces and the spring forces; the strength of the spring forces can be varied by several orders of magnitude without effecting the equilibrium position of the band.

Recently, an improved way of estimating the tangent to the elastic band at each image has been presented.[26] This eliminates a problem which occurred in systems where the force parallel to the MEP was very large compared with the restoring force perpendicular to the MEP.[9] In such situations kinks could form on the elastic band and prevent rigorous convergence to the MEP. We use this new way of estimating the tangent in the calculations presented here.

While the NEB method gives a discrete representation of the MEP, the energy of saddle points needs to be obtained by interpolation. When the energy barrier is narrow compared with the length of the MEP, few images land in the neighborhood of the saddle point and the interpolation can be inaccurate.

This communication describes a modification of the NEB method which gives a precise estimate of the saddle point at no extra cost as compared with the regular NEB.

II. DFT CALCULATIONS OF DISSOCIATIVE ADSORPTION

The method presented here has been applied to calculations of CH_4 dissociative adsorption on the Ir(111) surface and H_2 on the Si(100) surface using plane wave based density functional theory (DFT).[27] The PW91 functional[28,29] was used in combination with ultrasoft pseudopotentials.[30] The energy cutoff was 350 eV in the CH_4/Ir(111) calculation and 200 eV in the H_2/Si(100) calculation. The calculations were carried out with the VASP code[31] which we have extended to implement the new method presented here. The calculations were carried out in parallel on a cluster of workstations. The NEB method lends itself so well to parallel processing that it is sufficient to use a regular ethernet connection to transfer data between the nodes.

III. REGULAR NEB METHOD

An elastic band with $N+1$ images can be denoted by $[\mathbf{R}_0, \mathbf{R}_1, \mathbf{R}_2, \ldots, \mathbf{R}_N]$, where the end points, $\mathbf{R}_0$ and $\mathbf{R}_N$, are fixed and given by the energy minima corresponding to the initial and final states. The $N-1$ intermediate images are adjusted by the optimization algorithm.

In the NEB method,[9,26] the total force acting on an image is the sum of the spring force along the local tangent and the true force perpendicular to the local tangent

$$\mathbf{F}_i = \mathbf{F}_i^s|_{\parallel} - \nabla E(\mathbf{R}_i)|_{\perp}, \tag{2}$$

where the true force is given by

$$\nabla E(\mathbf{R}_i)|_{\perp} = \nabla E(\mathbf{R}_i) - \nabla E(\mathbf{R}_i)\cdot\hat{\boldsymbol{\tau}}_i. \tag{3}$$

Here, E is the energy of the system, a function of all the atomic coordinates, and $\hat{\boldsymbol{\tau}}_i$ is the normalized local tangent at image i. The spring force is

$$\mathbf{F}_i^s|_{\parallel} = k(|\mathbf{R}_{i+1}-\mathbf{R}_i| - |\mathbf{R}_i-\mathbf{R}_{i-1}|)\hat{\boldsymbol{\tau}}_i, \tag{4}$$

where k is the spring constant. An optimization algorithm is then used to move the images according to the force in Eq. (2). We have used a projected velocity Verlet algorithm.[9] The images converge on the MEP with equal spacing if the spring constant is the same for all the springs. Typically none of the images lands at or even near the saddle point and the saddle point energy needs to be estimated by interpolation.

An example of a NEB calculation is shown in Fig. 1. The MEP for dissociative adsorption of CH_4 on an Ir(111) surface has a narrow barrier compared with the length of the MEP. The molecule is 4 Å above the surface when the reaction coordinate is 1.0. At the other end, at 0.0, the molecule has broken up into a H and a CH_3 fragment sitting on adjacent on-top sites on the Ir(111) surface. The resolution of the MEP near the saddle point is poor and the estimate of the activation energy obtained from the interpolation is subject

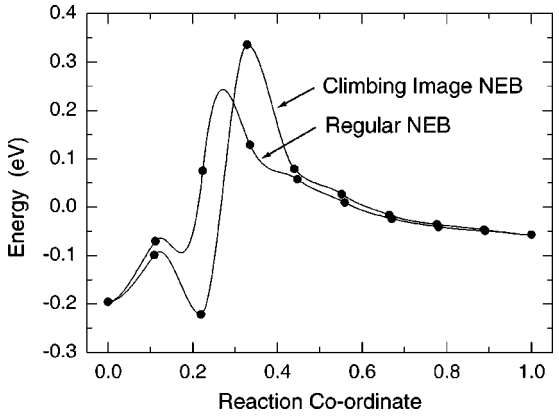

FIG. 1. Density functional theory calculations of the minimum energy path for CH_4 dissociative adsorption on a Ir(111) surface. The dissociated H and CH_3 fragments sitting on adjacent on-top sites correspond to reaction coordinate of 0.0. The CH_4 molecule 4 Å away from the surface corresponds to 1.0. A regular NEB calculation and a climbing image NEB calculation are compared, both involving 8 movable images. The regular NEB results in a low resolution of the barrier, and the interpolation gives an underestimate of the activation energy. The climbing image NEB brings one of the images right to the saddle point and gives the activation energy precisely with insignificant additional computational effort.

to large uncertainty. A force and energy based cubic polynomial interpolation was used between each pair of adjacent images. This is an example of a system where an intermediate minimum is located along the MEP. In fact, it turns out that this minimum is deeper than the chemisorbed state at the 0.0 end point. The configuration corresponding to the intermediate minimum has the adsorbed H atom at a bridge site.

IV. CLIMBING IMAGE NEB METHOD

The climbing image NEB (CI-NEB) method constitutes a small modification to the NEB method. Information about the shape of the MEP is retained, but a rigorous convergence to a saddle point is also obtained. This additional feature does not add any significant computational effort. After a few iterations with the regular NEB, the image with the highest energy $i_{\max}$ is identified. The force on this one image is not given by Eq. (2) but rather by

$$\begin{aligned}\mathbf{F}_{i_{\max}} &= -\nabla E(\mathbf{R}_{i_{\max}}) + 2\nabla E(\mathbf{R}_{i_{\max}})\big|_{\parallel} \\ &= -\nabla E(\mathbf{R}_{i_{\max}}) + 2\nabla E(\mathbf{R}_{i_{\max}})\cdot\hat{\boldsymbol{\tau}}_{i_{\max}}\hat{\boldsymbol{\tau}}_{i_{\max}}. \end{aligned} \tag{5}$$

This is the full force due to the potential with the component along the elastic band inverted. The maximum energy image is not affected by the spring forces at all.

Qualitatively, the climbing image moves up the potential energy surface along the elastic band and down the potential surface perpendicular to the band. The other images in the band serve the purpose of defining the one degree of freedom for which a maximization of the energy is carried out. Since the images in the band eventually converge to the MEP, they give a good approximation to the reaction coordinate around the saddle point. As long as the CI-NEB method converges, the climbing image will converge to the saddle point. Since all the images are being relaxed simultaneously, there is no additional cost of turning one of the images into a climbing image.

The results of a CI-NEB calculation of the CH_4 dissociation on Ir(111) is shown in Fig. 1. A significantly higher estimate of the activation energy is obtained than with the regular NEB, using the same number of images. The computational effort is the same to within 10% (CI-NEB not necessarily being slower). Alternatively, one could have run a second elastic band between the two images adjacent to the barrier to get a better estimate of the saddle point energy from the regular NEB, but this would have required more force evaluations and, therefore, more computational effort. The activation energy predicted by the DFT/PW91 calculations is approximately 0.4 eV. This calculation still needs to be corrected[33] for quantum zero point energy, dispersion, and system size effects before it can be compared to the experimental value[32] of 0.28 eV. The MEP is nontrivial because it involves a large relaxation of the substrate. The Ir atom closest to the CH_4 molecule in the transition state is pulled out from the surface plane by 0.5 Å. This means that the saddle point does not lie close to the straight line interpolation between the two end points. A more detailed presentation of the DFT calculations and comparison with experimental results will be given elsewhere.[33]

The climbing image is not affected by the spring forces. Therefore, the spacing of the images will be different on each side of the climbing image. As it moves up to the saddle point, images on one side will get compressed, and on the other side spread out. Two or more climbing images can be specified if the MEP appears to have two or more high maxima that are close in energy. The only issue is to have enough images close to the climbing image(s) to get a good estimate of the reaction coordinate, since this determines the climbing direction.

V. VARIABLE SPRING CONSTANTS

Since the saddle point is the most important point along the MEP, one would typically prefer to have more resolution in the MEP close to the saddle point than near the end points. The important issue is to get a good enough estimate of the tangent to the path near the saddle point, especially when a climbing image is included. As the images are brought closer to the saddle point, the approximation of the tangent will become more accurate. Dissociative adsorption of a molecule on a surface is an example of a process where the MEP is often highly asymmetric and the barrier region is only a small fraction of the MEP (see Figs. 1 and 2). In such cases, it is more efficient to distribute the images unevenly along the MEP.

This can be accomplished by using stronger springs near the saddle point. Because of the nudging, there is no interference between the spring forces that distribute the images along the MEP and the true force that brings the elastic band to the MEP. One is, therefore, free to choose different spring constants between different pairs of images without affecting the convergence of the band to the MEP, as long as the number of images is high enough. We have used a scheme where the spring constant depends linearly on the energy of the images, in such a way that images with low energy get connected by a weaker spring constant

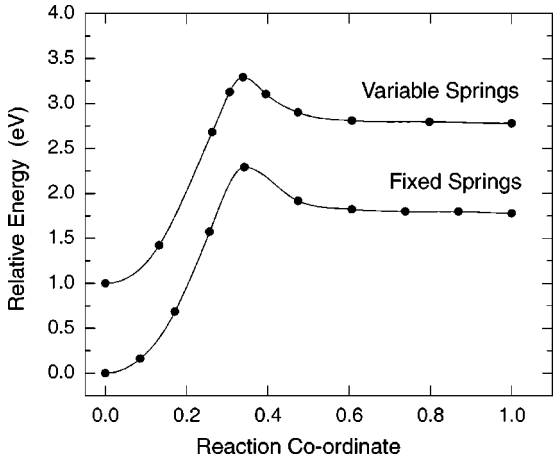

FIG. 2. Density functional theory calculations of the minimum energy path for H_2 dissociative adsorption on a Si(100) surface. The H adatoms sitting on adjacent Si atoms in a surface dimer correspond to reaction coordinate of 0.0. The H_2 molecule 3.8 Å away from the surface corresponds to 1.0. A regular climbing image NEB calculation with equal spring constants (curve labeled ''Fixed Springs'') is compared with a calculation where the spring constants are scaled with the energy (curve labeled ''Variable Springs,'' arbitrarily shifted by 1.0 eV). Both calculations involve 8 movable images. The variable spring calculation results in a higher resolution of the barrier with insignificant additional computational effort.

$$k_i' = \begin{cases} k_{\max} - \Delta k \left(\dfrac{E_{\max} - E_i}{E_{\max} - E_{\mathrm{ref}}} \right) & \text{if } E_i > E_{\mathrm{ref}} \\ k_{\max} - \Delta k & \text{if } E_i < E_{\mathrm{ref}}. \end{cases} \tag{6}$$

Here, $E_i = \max\{E_i, E_{i-1}\}$ is the higher energy of the two images connected by spring i, $E_{\max}$ is the maximum value of E_i for the whole elastic band, and E_{ref} is a reference value for the energy, defining a minimum value of the spring constant. We have chosen E_{ref} to be the energy of the higher energy endpoint of the MEP. This choice ensures that the density of images is roughly equal near the two end points, even for highly asymmetric MEPs. The spring constant is, therefore, linearly scaled from a maximum value $k_{\max}$ for highest energy images to a minimum value $k_{\max} - \Delta k$ for images with energy of E_{ref} or lower.

By choosing E_i to be the higher energy of the two images connected by the spring, the two images adjacent to the climbing image will tend to be symmetrically arranged around the saddle point. This is only approximately true because of the compression/stretching of the band on each side of the climbing image.

Figure 2 shows results of a calculation of the dissociation of a H_2 molecule on the Si(100) surface. This is an interesting system because of a long standing discrepancy[34] between experimental and theoretical measurements of adsorption and dissociation barriers. A CI-NEB calculation with equal spring constants is compared with a CI-NEB calculation with variable spring constants. The part of the MEP where the H_2 molecule approaches the Si(100) surface is flat and rather uninteresting. The energy scaling of the spring constants results in images being pulled up towards the barrier region, thus increasing the resolution of the MEP near the saddle point at the expense of the less important regions.

The number of force evaluations required to reach convergence to within a tolerance of 0.03 eV/Å was 179 for the regular NEB method (first 13 iterations with a small time step until the magnitude of the force had dropped below 1 eV/Å and then 166 iterations with a larger time step in the projected velocity Verlet algorithm[9]). The number of force evaluations needed for the CI-NEB calculation with equal spring constants was 190, and the number of force evaluations needed for the CI-NEB calculation with variable spring constants was 178. The difference between these numbers is not significant but simply reflects slight variations in the way the system moves on the energy surface towards the MEP.

ACKNOWLEDGMENTS

This work was funded by the National Science Foundation Grant No. CHE-9710995 and by the Petroleum Research Fund Grant No. PRF#32626-AC5/REF#104788.

[1] H. Eyring, J. Chem. Phys. **3**, 107 (1935).
[2] E. Wigner, Trans. Faraday Soc. **34**, 29 (1938).
[3] J. C. Keck, Adv. Chem. **13**, 85 (1967).
[4] P. Pechukas, in *Dynamics of Molecular Collisions*, edited by W. H. Miller (Plenum, New York, 1976), Part B.
[5] A. F. Voter and J. D. Doll, J. Chem. Phys. **80**, 5832 (1984); **82**, 80 (1985).
[6] C. Wert and C. Zener, Phys. Rev. **76**, 1169 (1949).
[7] G. H. Vineyard, J. Phys. Chem. Solids **3**, 121 (1957).
[8] M. L. McKee and M. Page, *Reviews in Computational Chemistry*, edited by K. B. Lipkowitz and D. B. Boyd (VCH, New York, 1993), Vol. IV.
[9] H. Jónsson, G. Mills, and K. W. Jacobsen, ''Nudged elastic band method for finding minimum energy paths of transitions,'' in *Classical and Quantum Dynamics in Condensed Phase Simulations*, edited by B. J. Berne, G. Ciccotti, and D. F. Coker (World Scientific, Singapore, 1998), p. 385.
[10] G. Henkelman, G. Jóhannesson, and H. Jónsson, ''Methods for finding saddle points and minimum energy paths,'' in *Progress on Theoretical Chemistry and Physics*, edited by S. D. Schwartz (Kluwer Academic, New York, 2000) (in press).
[11] G. Mills and H. Jónsson, Phys. Rev. Lett. **72**, 1124 (1994).
[12] G. Mills, H. Jónsson, and G. K. Schenter, Surf. Sci. **324**, 305 (1995).
[13] B. P. Uberuaga, M. Levskovar, A. P. Smith *et al.*, Phys. Rev. Lett. **84**, 2441 (2000).
[14] J. Song, L. R. Corrales, G. Kresse, and H. Jónsson, Phys. Rev. B (submitted).
[15] W. Windl, M. M. Bunea, R. Stumpf *et al.*, Phys. Rev. Lett. **83**, 4345 (1999).
[16] R. Stumpf, C. L. Liu, and C. Tracy, Phys. Rev. B **59**, 16047 (1999).
[17] T. C. Shen, J. A. Steckel, and K. D. Jordan, Surf. Sci. **446**, 211 (2000).
[18] M. Villarba and H. Jónsson, Surf. Sci. **317**, 15 (1994).
[19] M. Villarba and H. Jónsson, Surf. Sci. **324**, 35 (1995).
[20] E. Batista and H. Jónsson, *Computational Materials Science* (in press).
[21] M. R. Sørensen, K. W. Jacobsen, and H. Jónsson, Phys. Rev. Lett. **77**, 5067 (1996).
[22] T. Rasmussen, K. W. Jacobsen, T. Leffers *et al.*, Phys. Rev. Lett. **79**, 3676 (1997).
[23] R. Elber and M. Karplus, Chem. Phys. Lett. **139**, 375 (1987).
[24] R. Czerminski and R. Elber, Int. J. Quantum Chem. **24**, 167 (1990); J. Chem. Phys. **92**, 5580 (1990).
[25] R. E. Gillilan and K. R. Wilson, J. Chem. Phys. **97**, 1757 (1992).
[26] G. Henkelman and H. Jónsson, J. Chem. Phys. **113**, 9978 (2000), this issue.
[27] P. Hohenberg and W. Kohn, Phys. Rev. **136**, B864 (1964); W. Kohn and L. J. Sham, Phys. Rev. **140**, A1133 (1965).
[28] W. Kohn, A. D. Becke, and R. G. Parr, J. Phys. Chem. **100**, 12974 (1996).
[29] J. P. Perdew, in *Electronic Structure of Solids*, edited by P. Ziesche and H. Eschrig (Akademie, Berlin, 1991).
[30] D. Vanderbilt, Phys. Rev. B **41**, 7892 (1990).
[31] G. Kresse and J. Hafner, Phys. Rev. B **47**, 558 (1993); **49**, 14251 (1994); G. Kresse and J. Furthmüller, Comput. Mater. Sci. **6**, 16 (1996); Phys. Rev. B **54**, 11169 (1996).
[32] D. C. Seets, C. T. Reeves, B. A. Ferguson *et al.*, J. Chem. Phys. **107**, 10229 (1997).
[33] G. Henkelman and H. Jónsson (in preparation).
[34] F. M. Zimmermann and X. Pan, Phys. Rev. Lett. **85**, 618 (2000).